Partial duration series distributions of the European dry spell lengths for the second half of the twentieth century

C. Serra [1]

AQ2

Xavier Lana [1,*]

A. Burgueño [2]

M. D. Martínez [3]

[1] Departament de Física i Enginyeria Nuclear, Universitat Politècnica de Catalunya, Av. Diagonal 647, 08028 Barcelona, Spain

[2] Departament d'Astronomia i Meteorologia, Universitat de Barcelona, Martí Franquès 1, 08028 Barcelona, USA

[3] Departament de Física Aplicada, Universitat Politècnica de Catalunya, Av. Diagonal 649, 08028 Barcelona, USA

Abstract

A spatial analysis of partial duration series, PDS, of the dry spell lengths, DSL, is applied to 267 European stations during years 1951–2000. A DSL is defined as the number of consecutive days with precipitation below 0.1 mm/day. For every station, PDS are made of DSL longer than those corresponding to 95th empirical percentile. The L-skewness and L-kurtosis diagram of the PDS distributions shows that most of the stations fit well a generalised Pareto, GP, model. Only four rain gauge records at the southeast Mediterranean coast notably depart from this model. In addition, DSL maps for return periods of 2, 5, 10, 25 and 50 years are introduced by taking into account GP parameters, which are estimated by fitting the GP distribution to

empirical PDS distributions of DSL. A comparative study with those obtained in a previous paper, for the whole DSL series and the corresponding best distribution model (Pearson type III), shows that the differences of DSL for the different return periods keep within ±10 % in most of rain gauges. Moreover, a principal component analysis, PCA, is applied to the four first L-moments of the 267 rain gauges. Then, a regionalization in 11 groups is obtained after the clustering process. Finally, a regional frequency analysis is attempted, being possible to assign a GP parent distribution with different parameters to 7 out of the 11 groups.

AQ3

1. Introduction

Recent studies of climatic change summarised in the Intergovernmental Panel on Climate Change (IPCC)-2013 confirm a clear trend toward more extreme meteorological phenomena in many regions of the world. Although droughts do not depict a significant global trend, periods with rain scarcity have increased in some parts of the world, affecting the socioeconomic activities, agriculture and hydrological policies, among others. In agreement with Hartmann et al. (2013), whereas drought has increased in the Mediterranean during the period 1951–2010, European areas approximately north of 40–45° N have positive trends on rain amounts within this period. Population growth on relatively crowded areas as, for instance, the Mediterranean region, combined with the just mentioned drought increase, could aggravate environmental and economic problems.

AQ4

One approach to the drought phenomenon, among others, is the analysis of the dry spells. In the last decades, numerous analyses related to dry spell lengths, DSL, have been applied in different regions, as the Iberian Peninsula (Martín-Vide and Gómez 1999; Vicente-Serrano 2003; Serra et al. 2006; Lana et al. 2006a, b, 2008a, b, Sánchez et al. 2011), Greece (Anagnostopoulou et al. 2003; Nastos and Zerefos 2009), Croatia (Cindrić et al. 2010), Eastern Mediterranean (Kutiel 1985; Kostopoulou and Jones 2005), Italy (Brunetti et al. 2002), Switzerland (Schmidli and Frei 2005), France (Galloy et al. 1982; Douguédroit 1987), Belgium (Berger and Goossens 1983), Norway (Perzyna

1994), Brazil (Carvalho et al. 2013), Iran (Sarhadi and Heydarizadeh 2014), Argentina (Llano and Penalba 2011), USA (Groisman and Knight 2008), China (Gong et al. 2005; She et al. 2013), Europe (Heinrich and Gobiet 2011; Serra et al. 2013, 2014; Zolina et al. 2013) and West Africa (Sivakumar 1992), among others.

AQ5

The main objective of this study is to analyse the statistics and the spatial patterns of the partial duration series, PDS, of the DSL in Europe. The PDS strategy, also named peak over threshold, POT, has merited the acceptance of the hydrological community during last decades (Ben-Zvi 2009; Mailhot et al. 2013), with a solid theoretical basis developed in Coles (2001). Whereas this strategy consists on the selection of DSLs longer than a specific threshold, the annual extreme strategy, AES, only selects the longest dry spell every year. As a rule, the generalised Pareto, GP, distribution usually models PDS, while the generalised extreme value, GEV, distribution commonly models the annual extreme series, AES (Davison and Smith 1990). Studies by Madsen et al. (1997a, b) show that the PDS-GP approach is generally more efficient than the AES-GEV model. Other statistical models have been also applied, as the Weibull and log-normal distributions (Miquel 1984; Rosjberg et al. 1991; Ekanayake and Cruise 1993).

In the present manuscript, the GP distribution is applied for the PDS of the DSL, after contrasting this model with other statistical distributions. The GP parameters are estimated by L-moments (Hosking and Wallis 1997), taking advantage of their robustness to the effects of data outliers in comparison with conventional moments. It is worth to mention that other estimation methods (maximum likelihood, moments, probability weighted moments and generalised probability weighted moments) have been also proposed (Ashkar and Tatsambon 2007).

The selection of the appropriate truncation value to obtain the set of long and independent PDS events remains an open question (Beguería 2005; Ben-Zvi 2009; Mailhot et al. 2013). A common truncation threshold for Europe, whatever the rain gauge considered, is justified in the manuscript. This strategy has been previously applied in the PDS analysis of DSL in Catalonia (NE Spain) and in the Iberian Peninsula (Lana et al. 2006a, b). Leander et al. (2014) have

also applied the same threshold to analyse the contribution of very wet days to the total precipitation in Europe.

The contents of the paper are as follows. Section 2 introduces the main patterns of the database and the methodology of the statistical analysis. Section 3 summarises results concerning statistical models, return periods, clustering process and parent distributions. A discussion of the results is given in Section 4, and Section 5 summarises the main results.

2. Database and methodology

2.1. Database and dry spell length

Daily precipitation data for the years 1951–2000 have been compiled from 267 rain gauges in Europe. Most of these series (236) come from the European Climate Assessment and Dataset (ECA&D, http://eca.knmi.nl/). All these series are public and non-blended, and their quality has been analysed by ECA&D (Klein Tank et al. 2002; Wijngaard et al. 2003; Klok and Klein Tank 2009). The rest of series come from the *Agencia Estatal de Meteorología* (Spanish Ministry of Environment), which applied standard homogeneity tests and quality controls. The Vonn-Neumann ratio test and the Kolmogorov-Zurbenko filter have been also applied (Lana et al. 2008b).

Figure 1 depicts the spatial distribution of the stations. Dense rain gauge coverage is observed in Western Europe, except for Italy, Great Britain and the north of the Scandinavian Peninsula, where this coverage is not so dense. Turkish and Israel gauges are also included, but they only provide a rough approach for these countries, because interpolation of scarce spatial data could generate computational artifacts leading to some unrealistic spatial patterns. All rain gauges have a minimum continuous recording period of 40 years, and the series are complete (50 years) for 102 out of 267 stations. Figure 2a shows the number of stations with complete annual recordings. Most of the data series are continuous for the period 1955–1990. The number of available records increases at the beginning (1951–1955) and diminishes, especially, at the end (1990–2000) of the recording period. If a dry spell is likely to be incomplete because of lack of record continuity, it is rejected. This does not constitute a relevant shortcoming on account of the large enough population of DSL obtained.

Figure 2b shows the distribution of the stations depending on the number of recording years without lack of data.

Fig. 1

Spatial distribution of the 267 rain gauges in Europe. Rain gauges with minimum daily rain amount exceeding 0.1 mm/day are represented by *solid circles*

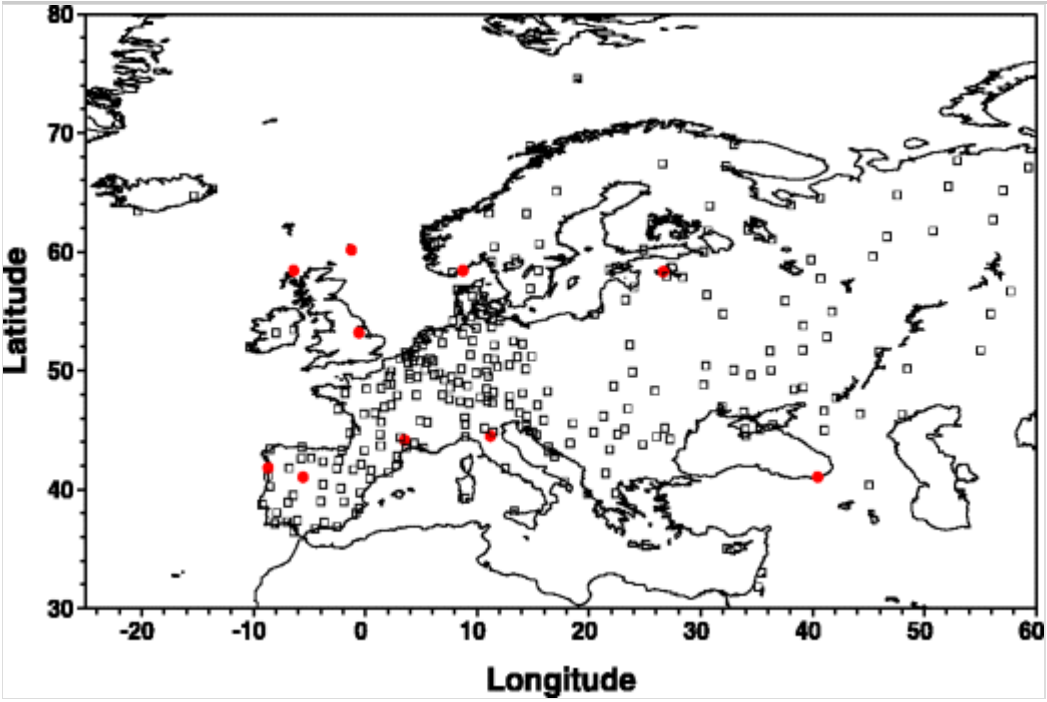

Fig. 2

a Number of available records per year along the recording period and **b** histogram of the number of stations depending on the number of recording years without lacking of data

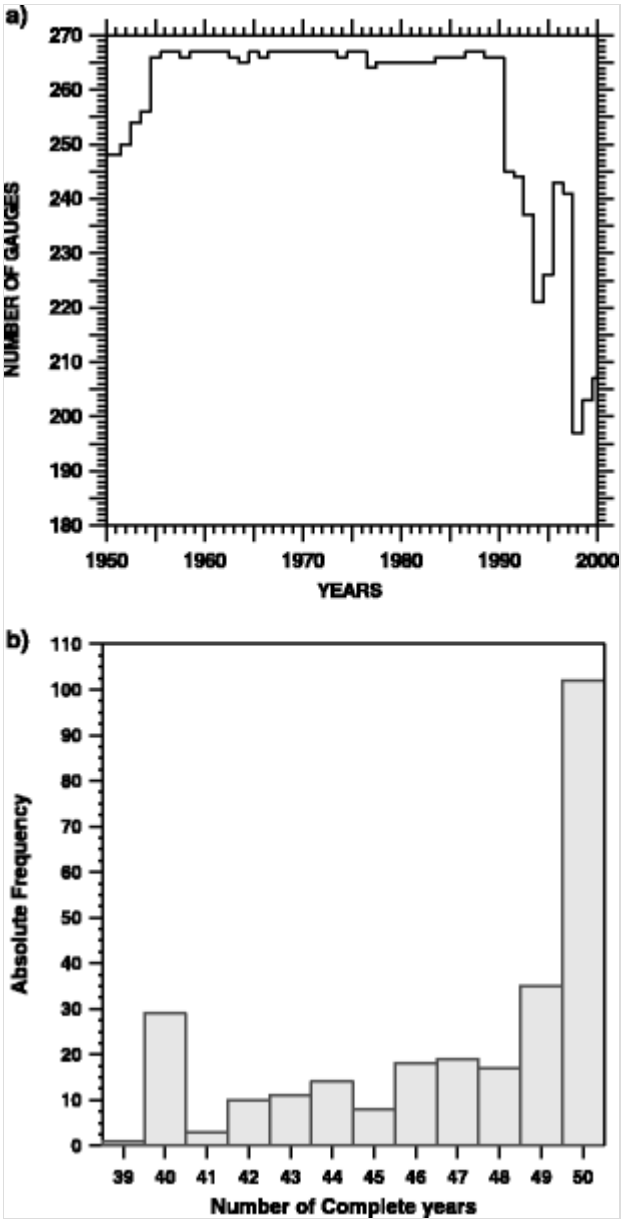

A DSL is defined as the length of a sequence of consecutive days with precipitation below a given threshold. Thresholds commonly used are 0.1, 1.0, 5.0 and 10.0 mm/day (Kutiel and Maheras 1992; Martín-Vide and Gómez 1999; Anagnostopoulou et al. 2003; Serra et al. 2006, 2013, 2014; Lana et al. 2008a, b; Cindrić et al. 2010). Whereas 0.1 mm/day is the usual lowest daily rain amount for a pluviometer, 1.0 and 5.0 mm/day are related to evapotranspiration and run-off processes, respectively, and, finally, 10.0 mm/day is related to saturation of thin surface layers (Lana et al. 2012). The study is limited in this paper to the threshold of 0.1 mm/day, with daily excess (shortage) defining a wet (dry) day. While most of the collected European series (257 out of 267 rain gauges) correspond to daily rainfall data recorded by pluviometers with minimum

daily rain amount of 0.1 mm/day, ten series (Fig. 1) are characterised by minimum daily rain amount exceeding 0.1 mm/day. The recorded minimum at Bologna (Italy) is 0.2 mm/day and nine pluviometers (three rain gauges at UK and one rain gauge in Estonia, France, Norway, Portugal, Spain and Turkey) have a recording minimum of 1.0 mm/day. The effects of the different minimum daily rain amounts on PDS statistics and return periods are discussed in Section 4. Figure 3a shows the spatial distribution of the 95th percentile, $L_{95\,\%}$, of the whole set of DSL. Additionally, the spatial distribution of the longest DSL for the whole recording period, $L_{\max}$, is plotted in Fig. 3b. Figure 3a, b shows very similar spatial patterns, with a clear dependence on latitude. Almost constant $L_{\max}$ at northern latitudes contrasts with increasing $L_{\max}$ for decreasing latitudes corresponding to the Mediterranean region. The longest $L_{\max}$ has been recorded at Har Kenaan (Israel) with 295 consecutive dry days in 1958. Other rain gauges with very high values are, for example, those from Cyprus, with 212 days; several ones at southern Spain, 170 days; Crete (south of Greece), 166 days; and Sicily (Italy), 116 days. Figure 3c and Table 1 summarise the distribution of rain gauges with $L_{\max}$ exceeding 90 days, being worth mentioning that all of them belong to the Mediterranean domain, south of 40° N. It is remarkable that the highest $L_{95\,\%}$ are located at the southeast of the Iberian Peninsula, in contrast with the highest $L_{\max}$ detected at the Eastern Mediterranean.

Fig. 3

a Ninety-fifth percentile of empirical DSL series. **b** The longest DSL for the whole recording period. **c** Rain gauges (*solid circles*) with $L_{\max}$ exceeding 90 days

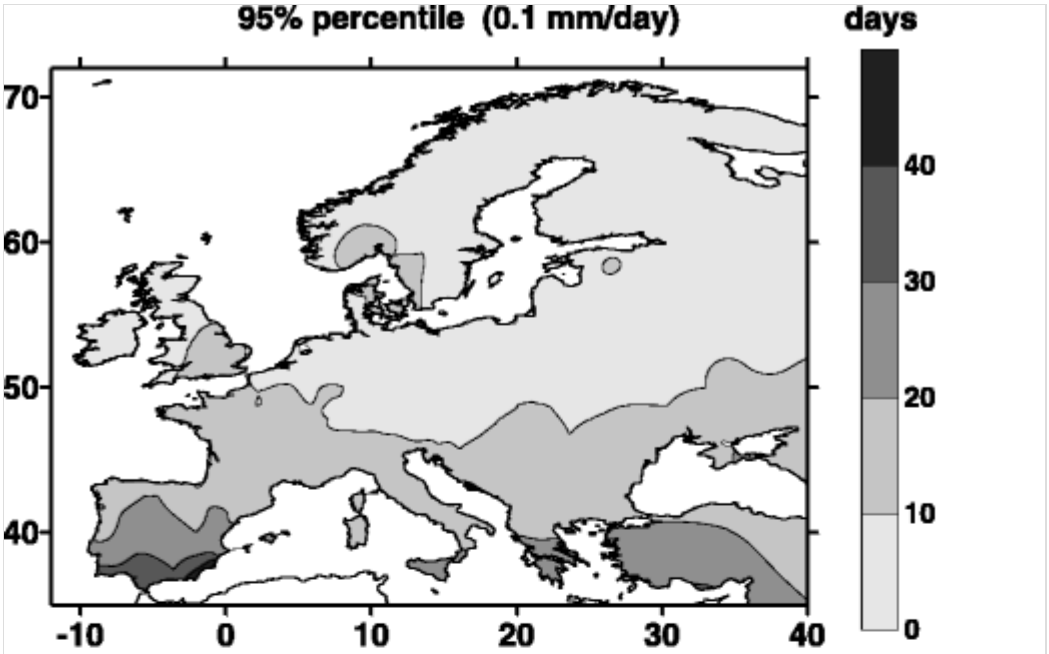
95% percentile (0.1 mm/day)
days
70
60
50
40
-10
0
10
20
30
40
0
10
20
30
40

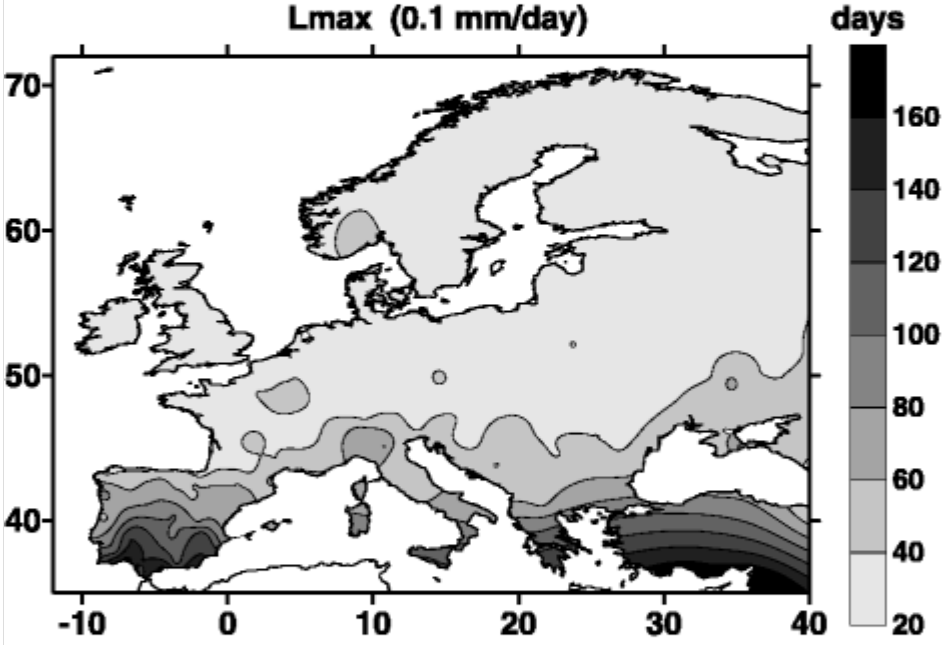
Lmax (0.1 mm/day)
days
70
60
50
40
-10
0
10
20
30
40
20
40
60
80
100
120
140
160

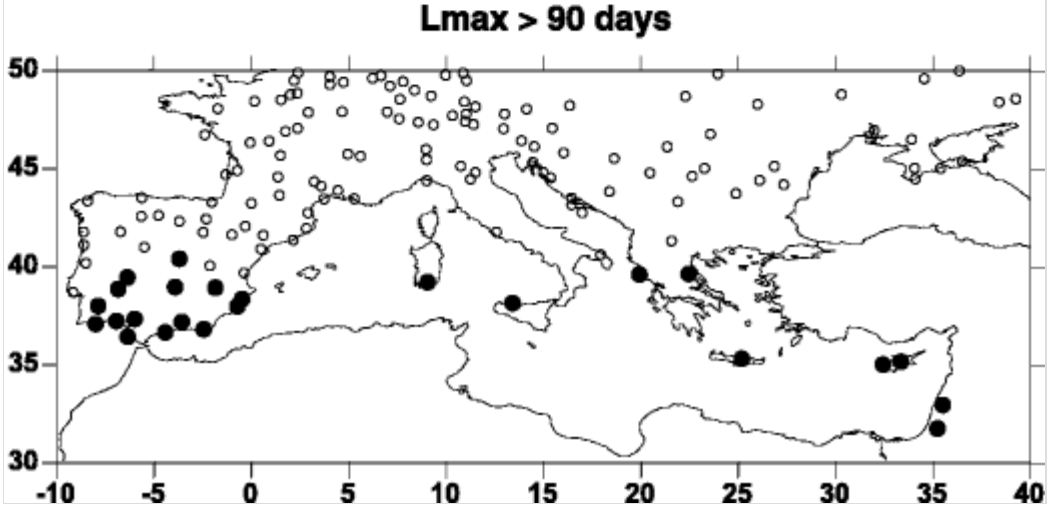
Lmax > 90 days
50
45
40
35
30
-10
-5
0
5
10
15
20
25
30
35
40

Table 1

Latitude, θ, longitude, λ, 95th percentile of DSL, $L_{95\ \%}$, and maximum recorded DSL, L_{max}, exceeding 90 days for rain gauges south of 40° N

Rain gauge	θ (°N)	λ (°E)	$L_{95\ \%}$	L_{max}
Har Kenaan (Israel)	32.97	35.50	28	295
Jerusalem (Israel)	31.77	35.22	28	215
Polis (Cyprus)	35.03	32.43	33	212
Nicosia (Cyprus)	35.17	33.35	33	179
Huelva (Spain)	37.25	−6.93	34	169
Malaga (Spain)	36.67	−4.42	40	169
Heraklion (Greece)	35.33	25.18	29	166
Almeria (Spain)	36.83	−2.45	44	156
Tavira (Portugal)	37.10	−8.00	39	155
Sevilla (Spain)	37.35	−6.00	34	140
Badajoz (Spain)	38.88	−6.84	28	139
Albacete (Spain)	38.95	−1.85	25	138
San Fernando (Spain)	36.45	−6.35	33	129
Caceres (Spain)	39.47	−6.37	28	126
Torrevieja (Spain)	38.00	−0.72	46	122
Palermo (Italy)	38.16	13.41	22	116
Granada (Spain)	37.20	−3.58	30	112
Beja (Portugal)	38.02	−7.87	26	106
Madrid (Spain)	40.42	−3.70	23	101
Larissa (Greece)	39.65	22.45	20	100
Alicante (Spain)	38.37	−0.48	28	96
Ciudad Real (Spain)	38.98	−3.92	26	96
Corfu (Greece)	39.62	19.92	21	95
Cagliari (Italy)	39.23	9.05	16	94

2.2. Partial duration series, PDS

PDS, made of lengths exceeding 95th percentile of DSL empirical distributions, are generated with the aim of obtaining the model describing better their cumulative probability distributions. The selection of the 95th percentile as general truncation level is based on the analysis of Lana et al. (2006a, b) for the Iberian Peninsula and northeastern Spain. In these papers, it was shown by means of excess plots (Beguería 2005) that the 95th percentile is a good common truncation value for these regions. At present, the excess plot method has been applied to define a truncation level for every DSL series. After analysing all the series, these levels are associated with probabilities within the 92nd–98th percentile range. It has been finally decided to accept a common truncation value of 95th percentile throughout Europe. As Fig. 3a shows, the highest thresholds for this percentile are obtained in the southeast of Spain (45 days).

The empirical L-skewness (t_3) and L-kurtosis (t_4) of the 267 PDS are obtained and represented in a diagram with different theoretical models, as Pearson type III (PE3), log-normal (LN), Weibull (WEI), GP, GEV and generalised logistic (GLO). The vicinity of the empirical distributions to each model is quantified in terms of the Euclidean distance, D, between analytical L-skewness, τ_3, and L-kurtosis, τ_4, generated as functions of the shape parameter and empirical L-skewness, t_3, and L-kurtosis, t_4 (Lana et al. 2006a, b)

$$D = \{ (t_3 - \ _3)^2 + (t_4 - \ _4)^2 \}^{1/2} \quad (1)$$

with the minimum D suggesting the best statistical distribution. This first evaluation of the goodness of fit is based on the fact that whatever the statistical model is tested, L-skewness (τ_3) and L-kurtosis (τ_4) only depend on the shape parameter (Hosking and Wallis 1997).

AQ6

AQ7

2.3. GP distribution

This distribution can be introduced as a function of three parameters: α (scale), κ (shape) and ξ (location) (Coles 2001). A reduced variable, y, of the original variable x, is defined as

$$y = -\frac{1}{}\ln\{1- \quad (x- \quad)/ \quad \}, \qquad 0 \tag{2}$$

and

$$y = (x- \quad)/ \quad , \qquad = 0 \tag{3}$$

describing the particular case of the exponential distribution. In terms of y, the GP distribution is given by

$$F(x; \quad , \quad , \quad) = 1 - \exp(-y) \tag{4}$$

The scale parameter α controls the spread of the observed distribution, in such a way that $F(x; \quad , \quad , \quad) = F(\frac{x}{} ; 1, \quad , \quad)$. Then, for larger (smaller) α, the observed distribution will be more spread out (concentrated). The location parameter ξ controls the position of the distribution function along the horizontal axis, being $F(x; \alpha, \kappa, \xi) = F(x - \xi; \alpha, \kappa, 0)$. And the shape parameter κ affects the shape of the distribution, rather than simply stretching it (as the scale parameter does) or shifting it (as the location parameter does).

In agreement with Hosking and Wallis (1997), the three parameters can be obtained from

$$= (1 - 3t_3)/(1 + t_3) \tag{5}$$

$$= (1 + \quad)(2 + \quad)_2 \tag{6}$$

$$= \quad _1 - (2 + \quad)_2 \tag{7}$$

with ℓ_1 and ℓ_2 as the two first empirical L-moments.

The goodness of fit of the empirical distribution to the GP model is evaluated by the Kolmogorov-Smirnov test. Ninety-five percent confidence bands are given by $\pm 1.36/N^{1/2}$ for a high enough number N of DSL. Then, a theoretical model $F(x)$ should be accepted if the empirical cumulative distribution is within the limits given by $F(x) \pm 1.36/N^{1/2}$ (Benjamin and Cornell 1970). This criterion must be carefully applied. When the empirical data used to compute L-moments and to estimate distribution parameters are also those used to apply the Kolmogorov-

Smirnov test, these confidence bands constitute only a rough approach and more sophisticated assessment techniques would be necessary for every specific distribution model (Lemeshko and Postokalov 2001). Nevertheless, taking into account that these assessment methods are easily applicable only for Gaussian distribution and the relatively small number of sample data (5 % of DSL), the 95 % confidence bands of the Kolmogorov-Smirnov test are finally applied.

2.4. Return periods for the PDS

A return DSL value, x_T (in days), for a return period T_r (in years), can be estimated according to:

$$T_r = 1/\{ (1 - F(x_T))\} \quad (8)$$

where β is the average number of DSL pertaining to the PDS per year, with different values for every rain gauge. This factor β is introduced so that the return period is given in years. Otherwise, T_r would be expressed in number of consecutive dry spells (Vicente-Serrano and Beguería 2003).

For the GP distribution, remembering Eqs. (2) to (4)

$$x_T = (/)\{1 - (T_r)^{-k}\} + \quad (9)$$

In agreement with Eq. (8), empirical values of x_T can be then obtained by searching for percentiles of

$$F(x_T) = 1 - 1/(T_r) \quad (10)$$

and taking into account that these cumulative probabilities are not 50, 80, 90, 96 and 98 %, corresponding to return periods, T_r, of 2, 5, 10, 25 and 50 years, but those linked to $\beta \cdot T_r$, in agreement with the definition given by Eq. (8). These empirical values can be then compared with theoretical x_T derived from Eq. (9), after estimation of parameters α, κ and ξ of the GP distribution.

2.5. Principal component analysis and clustering process

Before applying the clustering process for the regionalization, a principal component analysis, PCA, is applied to the original variables (Jolliffe 1986; Preisendorfer 1988). These original variables are the four empirical L-moments

$\{\ell_1\ ,\ \ell_2\ ,\ell_3\ ,\ \ell_4\}$ characterising every empirical PDS distribution. The orthogonal principal components, PCs, are standardised and ordered according to the amount of data variance they explain. PCs related to eigenvalues less than 1.0 are discarded in agreement with Dixon (1985), as they would explain less data variance than each one of the original variables. Additionally, orthogonal rotation of the components is applied for an easier interpretation of the PCs.

After the PCA, the clustering process, based on the average linkage, AL, algorithm (Kalkstein et al. 1987; Davis and Kalkstein 1990), is applied to the set of factor scores of the chosen PCs with the aim of obtaining coherent geographic regions from the viewpoint of PDS. The similarity index leading to determine the optimum number of clusters is defined as

$$L_{ij} = D_{ij}^2 + v_i + v_j \qquad 11$$

with D_{ij} the Euclidean distance between centroids of clusters i and j and v_i and v_j the corresponding within-group variances. L_{ij} systematically increases whatever the merged pair (i, j) of clusters. Then, in each step of the AL process, only the merging of the pair of clusters associated with the minimum increase of the similarity index is accepted. When an accepted merging of clusters is associated with a sharp increase on L_{ij}, the previous cluster configuration is chosen as the optimum and the clustering process finishes.

2.6. The regional frequency analysis and the parent distributions

After the clustering process, a regional frequency analysis (Hosking and Wallis 1997) is applied to the PDS. The main objective is to look for spatially coherent clusters of rain gauges with empirical PDS fitting well a single distribution, designed as parent distribution, which will be characterised by regional scale, shape and location parameters.

The cluster homogeneity parameter (Hosking and Wallis 1997; Tallaksen et al. 2004) is defined as

$$V_k = \frac{\sum_{j=1}^{N(k)} n_j \left(\tau_{2,j} - \tau_2^R \right)^2}{\sum_{j=1}^{N(k)} n_j} \right)^{1/2} \quad 12$$

$$\tau_2^R = \frac{\sum_{j=1}^{N(k)} n_j \tau_{2,j}}{\sum_{j=1}^{N(k)} n_i} \quad 13$$

where $N(k)$ is the number of rain gauges pertaining to the kth cluster, and n_j is the number of PDS elements of the jth rain gauge. $\tau_{2,j}$ is the L-moment coefficient of variation, L-CV, of the jth rain gauge and τ_2^R the regional L-moment for the kth cluster. V_k represents a weighted measure of the local $\tau_{2,j}$ dispersion with respect to the regional τ_2^R. After that, a Monte Carlo process may be applied to simulate random PDS for every rain gauge within the kth cluster, and the statistical significance of V_k is then validated (Lana et al. 2008a). Alternatively, the homogeneity of a cluster could be checked in terms of the quotient V_k/τ_2^R (Serra et al. 2013). A value of this quotient greater than 0.1 (10 % in percentage) would indicate heterogeneity of the PDS within the cluster and, consequently, a common parent distribution should be rejected. If the quotient is within the range 0.05–0.10 (5–10 %), the homogeneity of the cluster could be assumed as doubtful. Conversely, values of V_k/τ_2^R lower than 0.05 (5 %) would imply homogeneity of the PDS. Then, a parent distribution for all PDS belonging to the cluster, without distinguishing rain gauges, could be accepted and their regional parameters determined. Regional L-moments, including regional L-skewness and L-kurtosis, determined as weighted averages similar to Eq. (13), permit the estimation of regional scale, shape and location parameters (Eqs. 5, 6 and 7) of the assumed parent distribution.

AQ8

3. Results

3.1. The choice of the best distribution model

Figure 4 shows the L-skewness and L-kurtosis diagram corresponding to the 267 PDS. The GP appears as the best distribution model for the set of PDS. Nevertheless, four stations notably depart from this model. They are located in the southeast of the Mediterranean. Two of them, in Israel (Har Kenaan and Jerusalem), are closely distributed according to a GEV model. For the other two, in Cyprus and Crete Islands, the assignment of a specific distribution model is difficult. As a common feature, all of them are characterised by very long DSL. There are some rain gauges that, individually, fit slightly better other models such as WEI, PE3 or LN, for example, but they are also close to the GP model. Most of the rain gauges are close to the exponential model, represented by the crossing point of PE3, WEI and GP distribution curves. In short, if a single model should represent the probability distribution of the European PDS, this would be the GP model. According to Eq. (1), the minimum distances D between the empirical, t_3 and t_4, and the corresponding theoretical values, τ_3 and τ_4, correspond to the GP model, with an average value of 0.020 and a standard deviation of 0.017.

Fig. 4

L-skewness and L-kurtosis diagram for the empirical PDS of DSL and curves of *GP* (generalised Pareto), *GLO* (generalised logistic), *PE3* (Pearson type III), *GEV* (generalised extreme values), *LN* (log-normal) and *WEI* (Weibull) distributions

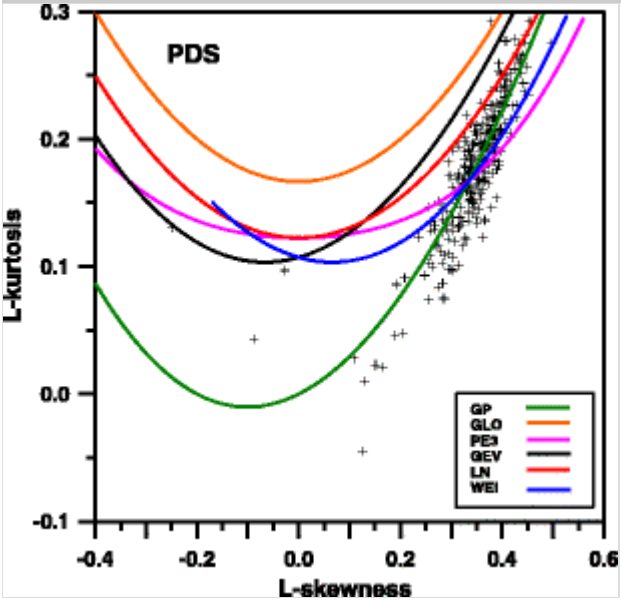

Figure 5 represents the spatial distribution of the three GP parameters, scale α,

shape κ and location ξ, for the PDS sampling strategy. The scale parameter, α, shows that most of European rain gauges have values lower than 20.0. A strong gradient appears in southern countries, especially in the vicinity of the Gulf of Cadiz (Iberian Peninsula) and in the Eastern Mediterranean coast. The highest α values are linked to a few stations, previously mentioned, departing from the GP model. Then, the reliability of these α values is debatable. A similar gradient is obtained for the shape parameter, κ. The values have a small range, from −0.2 to 0.2, for a great part of Europe. Some differences are observed for the location parameter, ξ, where the highest values are located in the southeast coast of the Iberian Peninsula. This spatial distribution is very similar to that of the 95th percentile of the whole set of DSL (Fig. 3a). In fact, parameter ξ represents the lowest value of the distribution or, in other words, the chosen PDS threshold. Given that the low density of rain gauges at the southeastern Mediterranean compared with the high density in the Iberian Peninsula, spatial gradients observed for the second case are more reliable than those detected for the first case, which could be questionable. Consequently, from the viewpoint of extreme DSL regimes, different climatic conditions for eastern and western Mediterranean cannot be absolutely assessed. Nevertheless, in agreement with Table 1, the longest DSL at the southeast always keep above those at western and central Mediterranean.

Fig. 5

Spatial distribution of parameters α (scale), κ (shape) and ξ (location) for the GP distribution

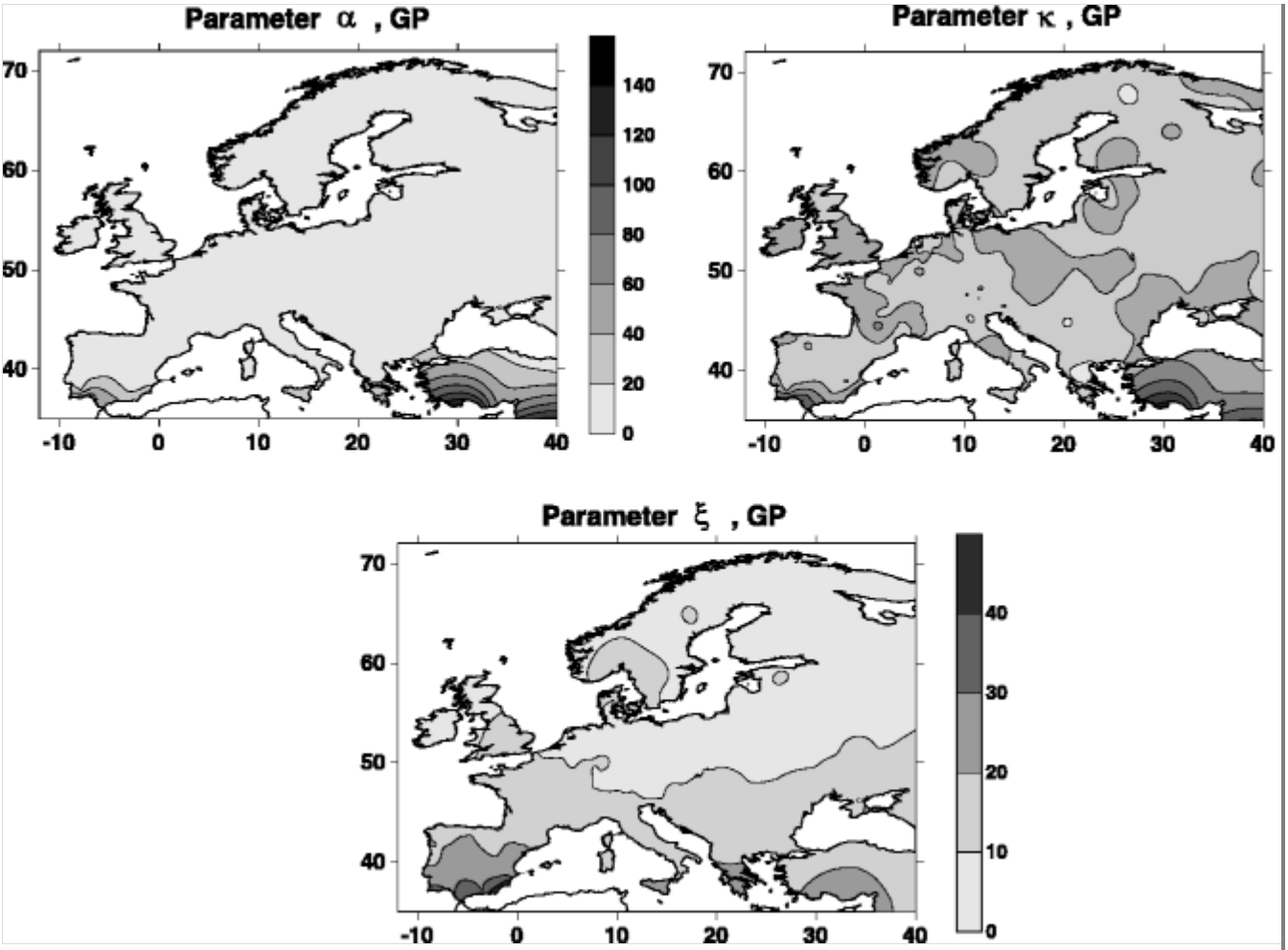

Figure 6a illustrates four examples of the fit obtained with the PE3 model for all dry spell, ADS, sampling strategy (Serra et al. 2013, 2014) and with the GP model for the PDS obtained here, including the 95 % confidence bands of the Kolmogorov-Smirnov test (Benjamin and Cornell 1970). The four examples are well fitted by both models, including the series of Almeria, at the southeast of Spain, in one of the driest European areas. It is worth mentioning that, although the confidence bands for the ADS strategy used to be very narrow due to the high number of observations, *N*, fits are reasonably good. Figure 6b corresponds to Har Kenaan, one of the four rain gauges with PDS departing significantly from the GP model. This distribution is quite different with respect to most of the European stations. Whereas the PDS distribution follows the GEV model, ADS series are roughly distributed according to GP model. The very different behaviour of this rain gauge could not be surprising bearing in mind its very low latitude (32, 9° N), in comparison with most of the European rain gauges considered and its arid climatic regime.

Fig. 6

a Four examples of ADS and PDS empirical distributions modelled by the PE3 and GP distributions, respectively. **b** ADS and PDS empirical distributions for Har Kenaan rain gauge, modelled by the GP and GEV distributions, respectively. *Dashed lines* represent the Kolmogorov-Smirnov 95 % confidence bands

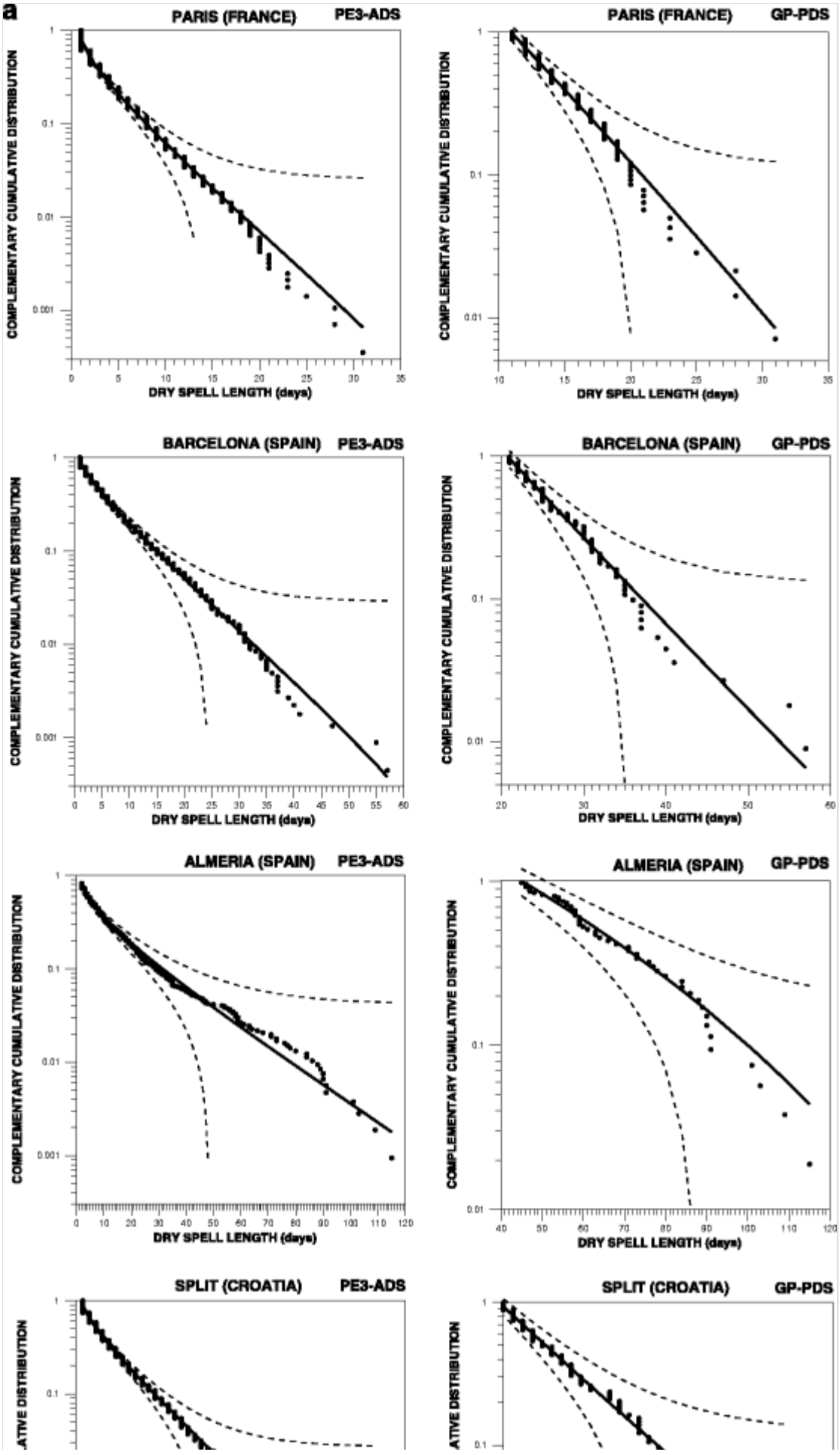
a
PARIS (FRANCE) PE3-ADS
PARIS (FRANCE) GP-PDS
BARCELONA (SPAIN) PE3-ADS
BARCELONA (SPAIN) GP-PDS
ALMERIA (SPAIN) PE3-ADS
ALMERIA (SPAIN) GP-PDS
SPLIT (CROATIA) PE3-ADS
SPLIT (CROATIA) GP-PDS
COMPLEMENTARY CUMULATIVE DISTRIBUTION
DRY SPELL LENGTH (days)

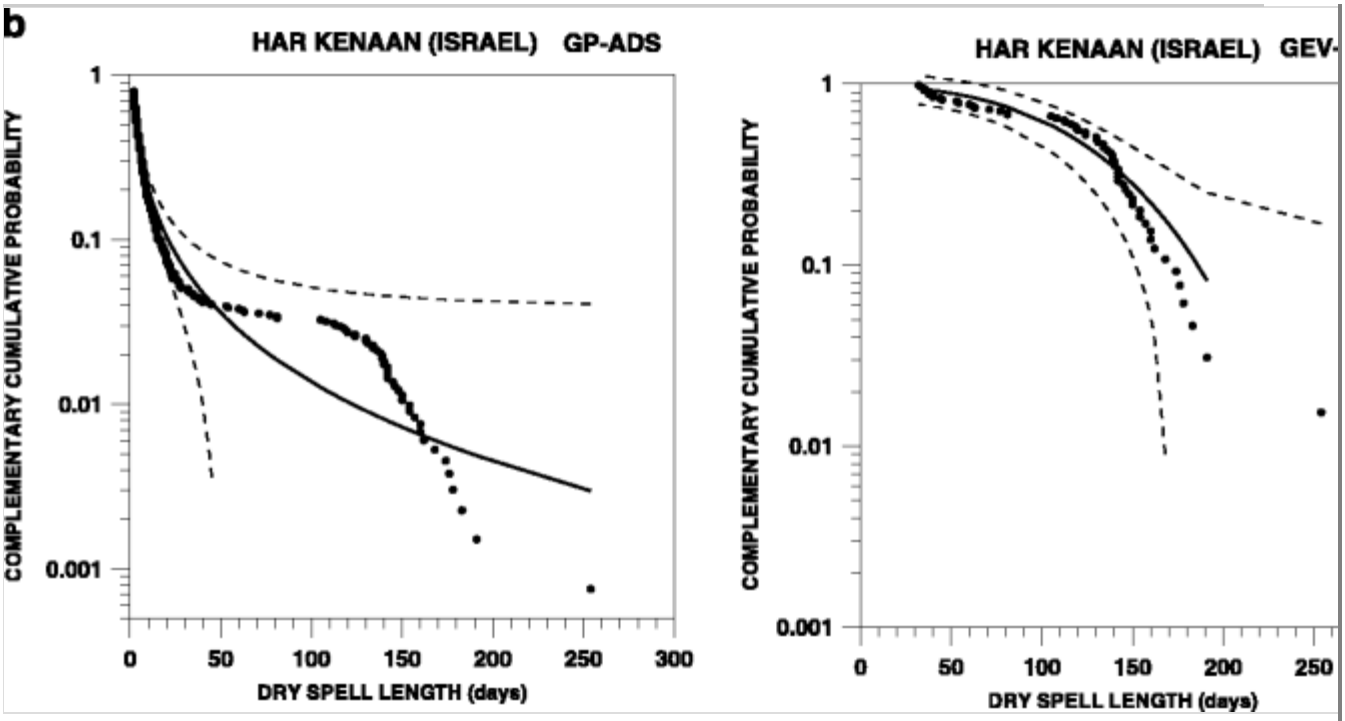

AQ9

3.2. Return periods

Figure 7 shows the spatial distribution of theoretical DSL for return periods of 2, 5, 10, 25 and 50 years, according to the GP model, together with the relative discrepancies between return periods derived from ADS (PE3 distributed) and from PDS (GP distributed), in agreement with Serra et al. (2013). The spatial patterns of the return values are very similar for both PDS and ADS, whatever the return period considered. Two different zones can be distinguished. While a spatial homogeneity is detected for latitudes north of 40–45° N, with a narrow range of return values, areas south of these latitudes show a remarkable increase of these values from north to south, suggesting much more variable regimes. Whereas for return periods of 2, 5 and 10 years most of northern Europe is characterised by DSLs exceeding 10–30 days, for southern territories, DSL can reach values exceeding 30–190 days. For the same territories of southern Europe and return periods of 25 and 50 years, DSL can exceed 50–290 days, with the highest values in the southeastern Mediterranean (Israel).

Fig. 7

a DSL for return periods of 2, 5, 10, 25 and 50 years from GP-PDS strategy. **b** Relative differences between DSL deduced from PE3-ADS and GP-PDS strategies, for the same return periods

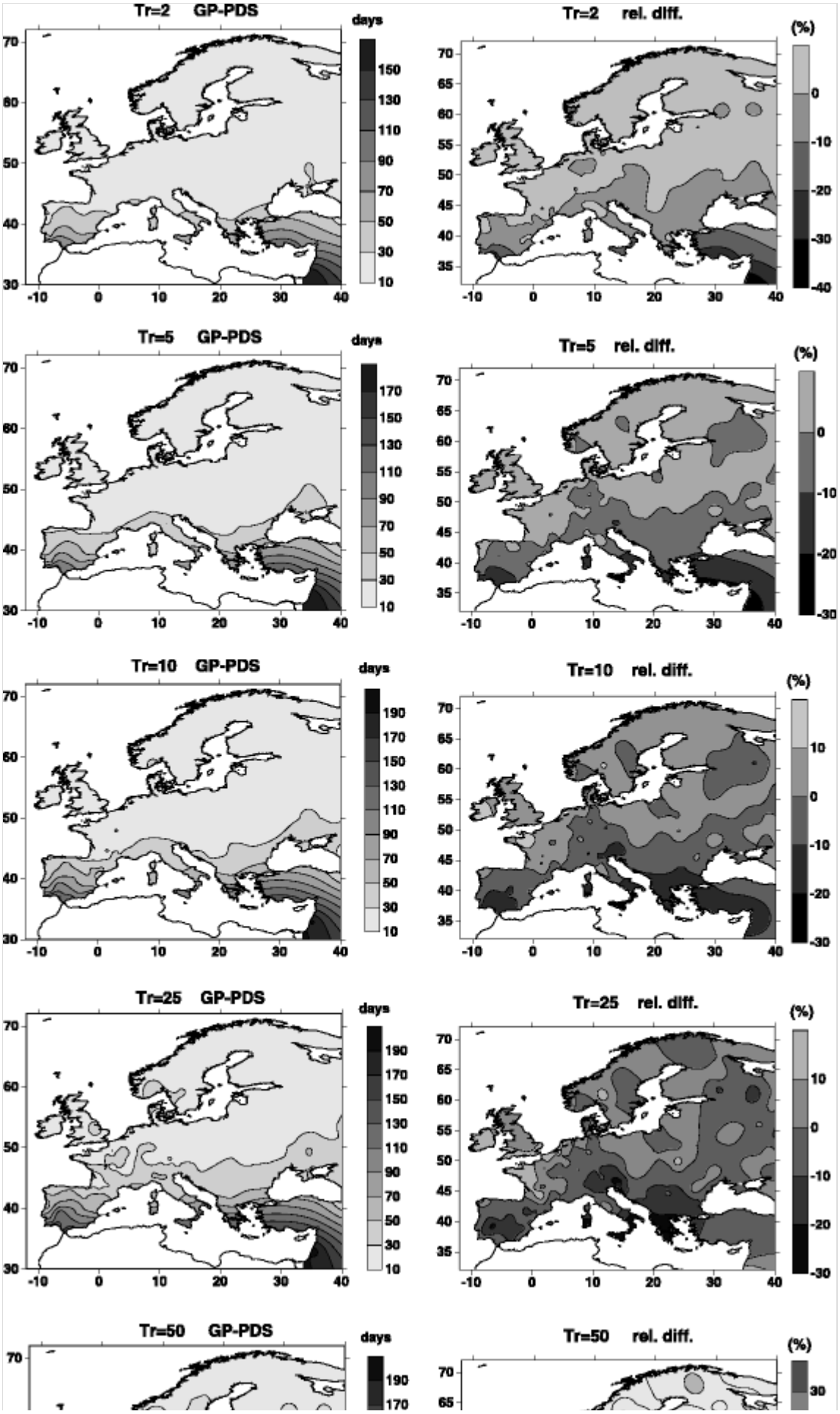
Tr=2 GP-PDS
days
150
130
110
90
70
50
30
10
Tr=2 rel. diff.
(%)
0
-10
-20
-30
-40
Tr=5 GP-PDS
days
170
150
130
110
90
70
50
30
10
Tr=5 rel. diff.
(%)
0
-10
-20
-30
Tr=10 GP-PDS
days
190
170
150
130
110
90
70
50
30
10
Tr=10 rel. diff.
(%)
10
0
-10
-20
-30
Tr=25 GP-PDS
days
190
170
150
130
110
90
70
50
30
10
Tr=25 rel. diff.
(%)
10
0
-10
-20
-30
Tr=50 GP-PDS
days
190
170
Tr=50 rel. diff.
(%)
30

Taking as reference the PDS strategy, the relative differences between ADS and PDS return values are given in percentage, being computed as ($DSL_{PE3\text{-}ADS} - DSL_{GP\text{-}PDS}$) × 100 / $DSL_{GP\text{-}PDS}$. For return periods of 2 and 5 years, the relative differences for a wide domain of Europe range within the (−10 %, +10 %) interval. Only a few rain gauges of the southern Mediterranean coast are characterised by relative differences from −20 up to −40 %. For return periods of 25 and 50 years, rain gauges located at the south and centre of the Iberian Peninsula, south of Italy and Greece, as well as other northern regions as for example Ireland, south England, Atlantic coast of France and the Alps, show very notable differences between return values according to ADS and PDS strategies. As an example, the return values of DSL (GP-PDS strategy) estimated for Greece could exceed by 30 or 40 days than those estimated for the PE3-ADS strategy.
AQ10

Figure 8 illustrates the relative differences (absolute values) between the empirical and theoretical DSL return values for the different return periods and ADS and PDS strategies, while Table 2 summarises the results. Systematically, for all return periods, relative differences are lower for the PDS, modelled by GP distribution, than for the ADS, modelled by PE3 distribution. For return periods of 2, 5 and 10 years, most of Europe shows absolute differences lower than 10 % for both models but especially for the GP-PDS strategy. As expected, the percentage of discrepancy between empirical and theoretical DSL return values increases for 25 and 50 years, whether ADS or PDS strategies are considered, and the spatial patterns of these discrepancies become more complex.

Fig. 8

Absolute relative differences between **a** empirical DSL and PE3-ADS values for return periods of 2, 5, 10, 25 and 50 years. **b** The same for empirical DSL and GP-PDS values

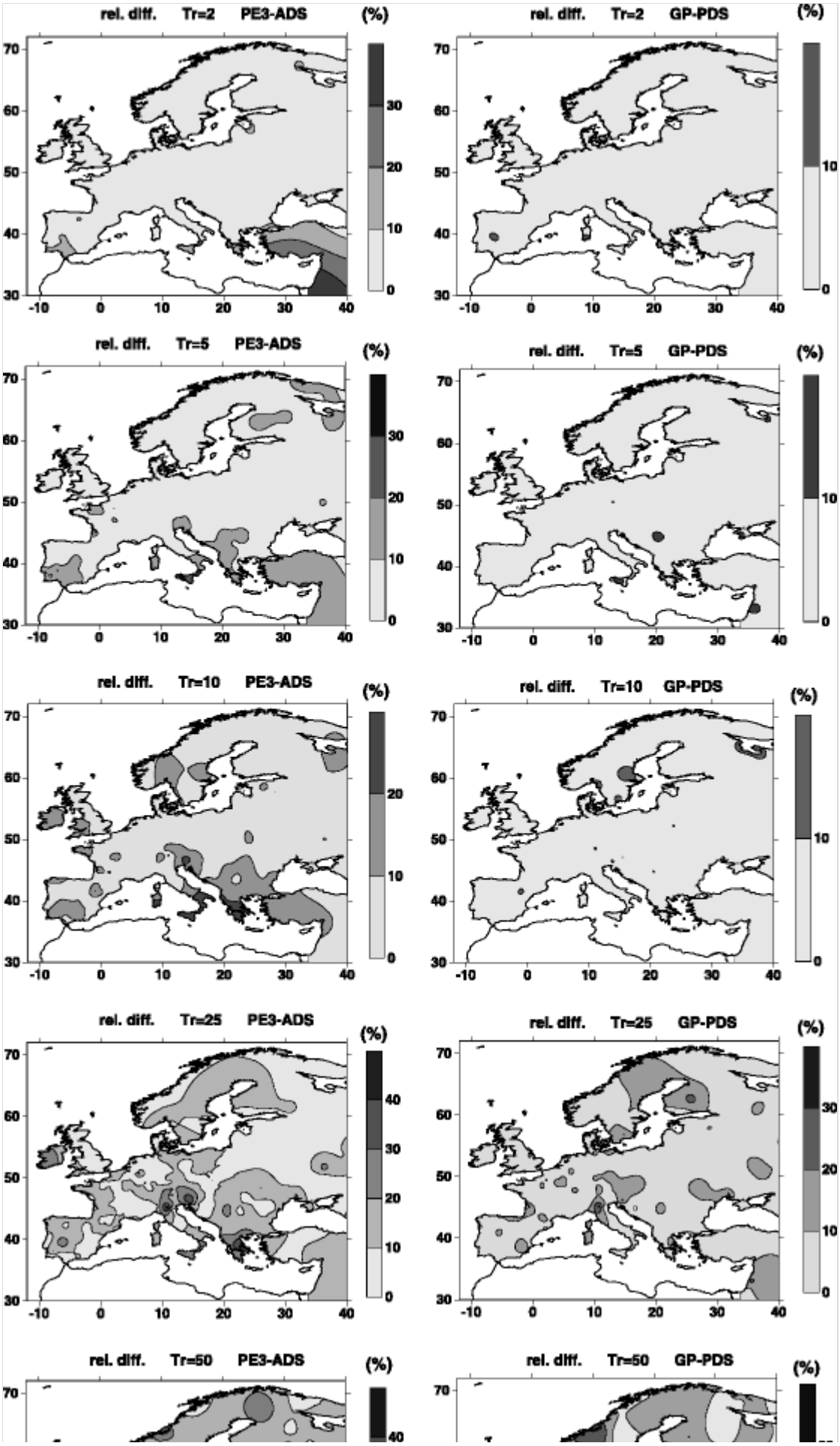
rel. diff. Tr=2 PE3-ADS
(%)
rel. diff. Tr=2 GP-PDS
(%)
rel. diff. Tr=5 PE3-ADS
(%)
rel. diff. Tr=5 GP-PDS
(%)
rel. diff. Tr=10 PE3-ADS
(%)
rel. diff. Tr=10 GP-PDS
(%)
rel. diff. Tr=25 PE3-ADS
(%)
rel. diff. Tr=25 GP-PDS
(%)
rel. diff. Tr=50 PE3-ADS
(%)
rel. diff. Tr=50 GP-PDS
(%)

Table 2

Absolute average, $<\varepsilon>$, and maximum, ε_{max}, relative differences between empirical and theoretical DSL, for ADS and PDS sample strategies and different return periods

T_r (years)	2	5	10	25	50
$<\varepsilon>_{ADS}$ (%)	4.6	6.2	7.1	10.7	14.3
$<\varepsilon>_{PDS}$ (%)	2.9	3.8	3.9	6.8	9.7
ε_{maxADS} (%)	38.3	30.6	27.2	45.3	46.2
ε_{maxPDS} (%)	15.8	13.6	17.0	33.0	35.1

AQ11

3.3. Principal component analysis, regionalization, and parent distributions

Table 3 shows the correlation between the original variables (the first four L-moments) and the first three rotated principal components, RPCs, derived from the PCA algorithm. The explained variance related to each of these RPCs and their eigenvalues are also included. RPC1 is highly correlated with the first and second L-moment, explaining 48.3 % of the total variance. RPC2 is very well correlated with the fourth L-moment and it explains the 25.9 %, and RPC3 correlates with the third L-moment, contributing with 25.2 %. As a summary, the three RPCs explain a high percentage (99.4 %) of the total data variance. The fourth principal component has not been considered given that its eigenvalue is less than 1.0, then explaining less data variance than an original L-moment.

Table 3

Correlation matrix between rotated principal components, RPCs, and the four L-moments $\{\ell_1, \ell_2, \ell_3, \ell_4\}$. The eigenvalue, EV, and the explained variance, Var., and cumulative variance, CVar. (in percentage), are also included for each RPC

AQ12

	RPC1	RPC2	RPC3
ℓ_1	**0.941**	0.315	0.064
ℓ_2	**0.961**	0.246	0.085

	RPC1	RPC2	RPC3
ℓ_3	0.076	0.068	**0.995**
ℓ_4	0.346	**0.935**	0.080
EV	1.933	1.038	1.007
Var. (%)	48.3	25.9	25.2
CVar. (%)	48.3	74.2	99.4

Figure 9 illustrates the spatial distribution of the factor scores, FS, corresponding to the three first rotated principal components, RPC1, RPC2 and RPC3. While RPC1 shows the maximum values of FS in the southwest of the Iberian Peninsula and south of Turkey, a great part of Europe has values close to zero. The highest values of FS linked to RPC2 correspond to inland Iberian Peninsula, south of Italy, middle Greece and Israel. The third principal component, RPC3, which explains almost the same variance than RPC2, is characterised by the maximum values of FS in the inland areas of the Iberian Peninsula, south of Italy, Greece and Cyprus.

Fig. 9

Spatial distribution of the factor scores, *FSs*, for the three first rotated principal components, *RPCs*

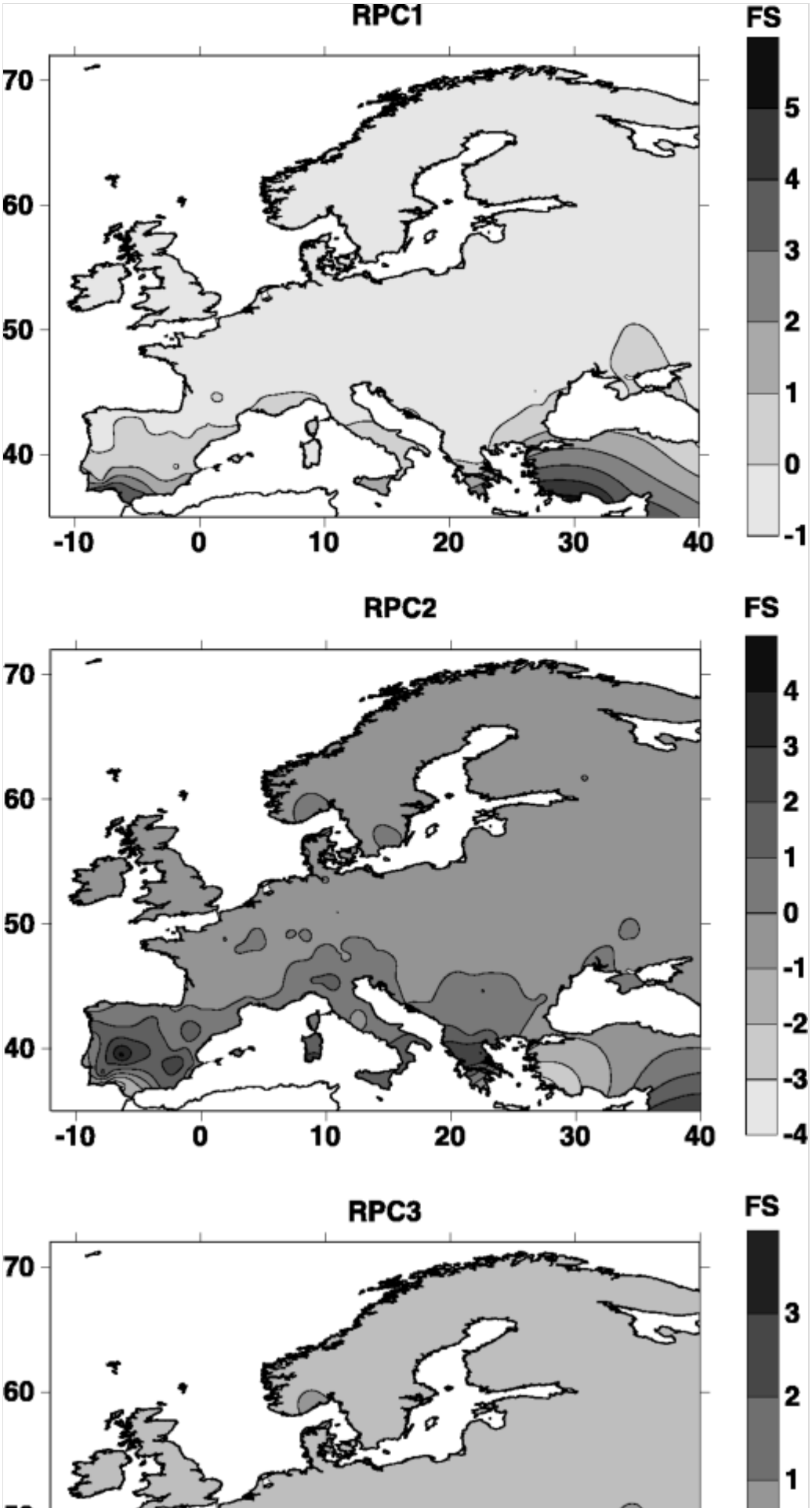
RPC1
FS
5
4
3
2
1
0
-1
70
60
50
40
-10
0
10
20
30
40
RPC2
FS
4
3
2
1
0
-1
-2
-3
-4
70
60
50
40
-10
0
10
20
30
40
RPC3
FS
3
2
1
70
60

The clustering process is applied to the FS of the RPCs by means of the average linkage method. Figure 10 shows the evolution of the similarity index with respect to the number of clusters. A first relatively abrupt change in the similarity index is observed when the number of clusters is reduced from 11 to 10. A second great change is also detected when the number of clusters is reduced from 7 to 6. The regionalization in 11 clusters has been finally chosen after an inspection of the spatial distribution of the groups and the number of rain gauges in each cluster.

Fig. 10

Evolution of the similarity index with the number of clusters. *Vertical arrows* indicate two acceptable configurations of 7 and 11 clusters

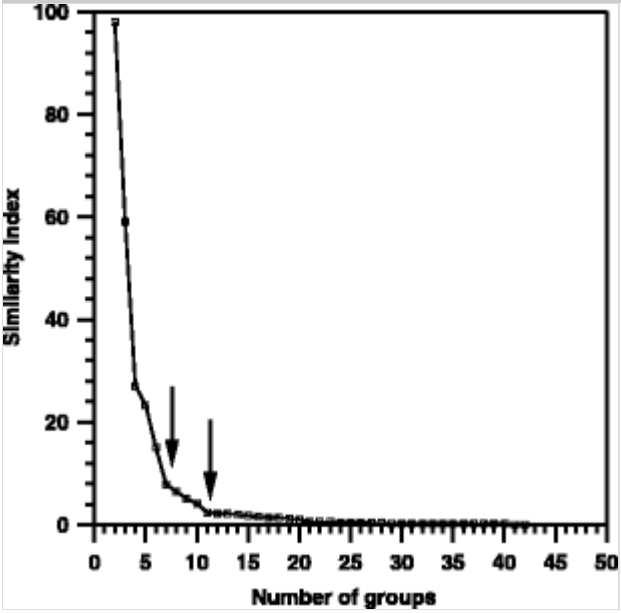

Figure 11 illustrates the cluster distribution, and Table 4 shows the main patterns of every cluster. Figure 12 depicts the regional third and fourth L-moments in the L-skewness and L-kurtosis diagram. Cluster 1 is a large group compounded by 241 rain gauges with latitudes north of 40° N. The regional parameters of this cluster are the smallest, and the regional L-skewness and L-kurtosis are close to the exponential point but compatible with the GP model (Fig. 12). The coefficient V_k/τ_2^R reaches a value equal to 9.1 %, which could be considered relatively small taking into account the numerous rain gauges belonging to this cluster. In short, this cluster could be qualified as relatively homogeneous, with a parent GP distribution describing the statistical

distribution of PDS for a great area of Europe.

Fig. 11

Regionalization of the European rain gauges for 11 clusters. The *dashed line* represents a schematic distinction between homogeneous and heterogeneous DSL regimes

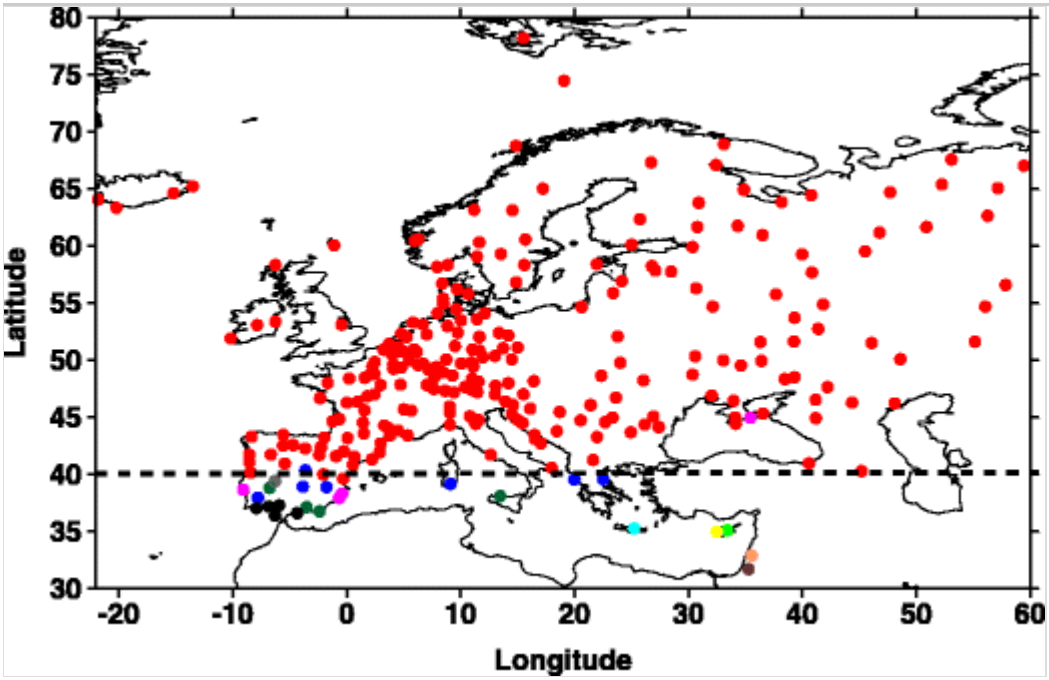

Table 4

Symbols used in Fig. 11 to identify clusters, number of rain gauges, Ns, for each group, Ng, the four regional $\{\ell_1, \ell_2, \ell_3, \ell_4\}$ L-moments, regional GP parameters (α, κ, ξ) and the homogeneity coefficient (V/τ_2)

Ng	Symbol	Ns	ℓ_1	ℓ_2	ℓ_3	ℓ_4	κ	α	ξ	V/τ_2
1		241	15.6	2.3	0.8	0.4	−0.045	4.4	11.0	9.1
2		1	77.0	20.9	4.1	1.0	0.319	63.8	28.6	
3		1	111.4	25.8	−2.3	1.1				
4		7	35.8	7.3	3.0	1.5	−0.155	11.4	22.4	6.4
5		1	82.2	24.8	3.1	−1.1				
6		1	116.6	30.3	−0.8	3.0				
7		1	135.3	28.1	−7.0	3.7				
8		4	47.2	7.9	2.1	0.8	0.153	19.6	30.2	9.8

Ng	Symbol	Ns	ℓ_1	ℓ_2	ℓ_3	ℓ_4	κ	α	ξ	V/τ_2
9		4	52.6	11.7	3.9	1.4	0.006	23.7	29.1	15.9
10		1	47.9	10.8	4.6	2.3	−0.196	15.6	28.5	
11		5	73.6	16.2	2.4	0.4	0.484	59.7	33.4	6.9

Fig. 12

Regional L-skewness and L-kurtosis values for the PDS of the 11 clusters and curves of *GP* (generalised Pareto), *GLO* (generalised logistic), *PE3* (Pearson type III), *GEV* (generalised extreme values), *LN* (log-normal) and *WEI* (Weibull) distributions

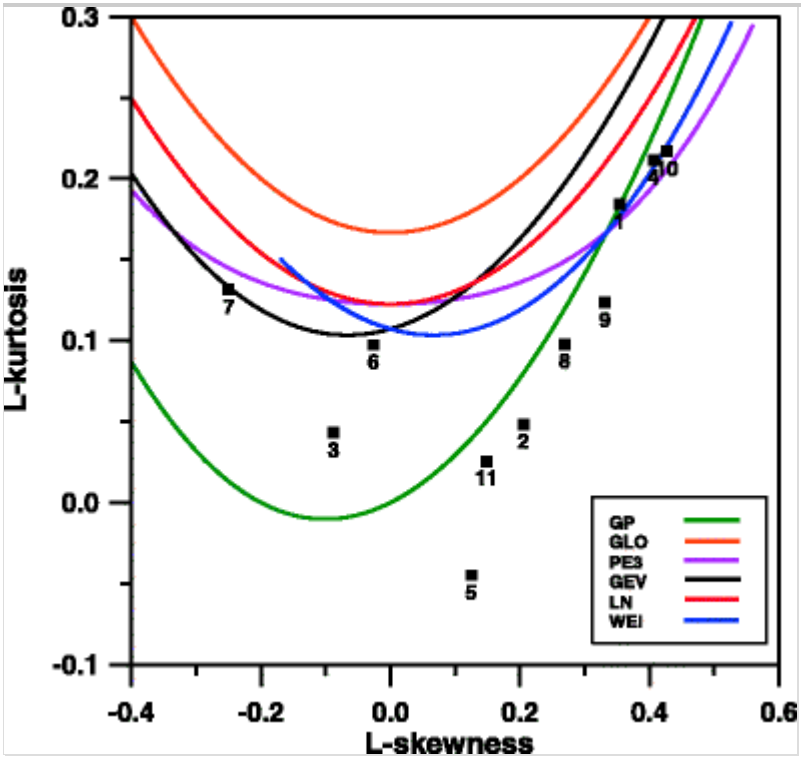

In the southern Mediterranean, clusters are small or singular, with a high variability of their regimes in comparison with the northern latitudes. While clusters 4 and 11 are the most homogeneous, with quotients V_k/τ_2^R lower than 7 %, cluster 9 is the less homogeneous, reaching a quotient of 15.9 %. Given that singular clusters 3, 5, 6 and 7 depart from the GP model, their distribution parameters are not included in Table 4. Single clusters 6 and 7, with the highest ℓ_1 , ℓ_2 and ℓ_4 L-moments and negative values of ℓ_3, are very close to the GEV model.

The parent distribution (Hosking and Wallis 1997; Tallaksen et al. 2004) is defined as a distribution function fitting PDS of DSL pertaining to all the rain gauges assigned to a cluster. As mentioned before, regional L-moments derived from these assembled data permit an estimation of a parent distribution, with specific regional scale, shape and location parameters, for every cluster. The different regional parent distributions of the GP model are represented in Fig. 13. These distributions have been obtained taking into account the GP regional parameters of Table 4. The singular groups departing from GP model are not included. As mentioned before, the parent distribution of cluster 1 is the closest to an exponential distribution. It is worth mentioning that whereas the longest expected DSL for cluster 1 is close to 50 days, for the rest of clusters, it exceeds 110 days, reaching very high lengths greater than 200 days (clusters 2 and 10).

Fig. 13

GP parent distributions for the seven indicated clusters

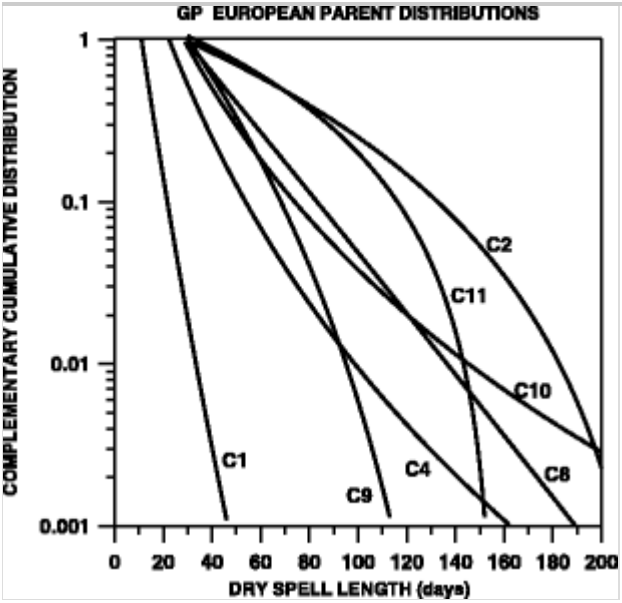

Finally, in order to confirm the contrast between the DSL regime at northern and southern latitudes, Fig. 14a represents the evolution of the L-moment coefficient of variation, L-CV or τ_2, with rain gauge latitudes. In this figure, it is easily observed that, for latitudes north of ≈45° N, τ_2 varies within a narrow range (0.13–0.18), and only for latitude south of ≈45° N, a linear increase with decreasing latitude is detected, in agreement with a larger variety of DSL patterns

for southern Europe. Conversely, Fig. 14b shows the lack of a clear relationship between τ_2 and rain gauge longitudes.

Fig. 14

Evolution of the L-coefficient of variation τ_2 (n-CV) for **a** the different latitudes and **b** longitudes of the rain gauges. The *straight line* represents the almost linear increase of τ_2 for decreasing latitudes south of ≈45° N

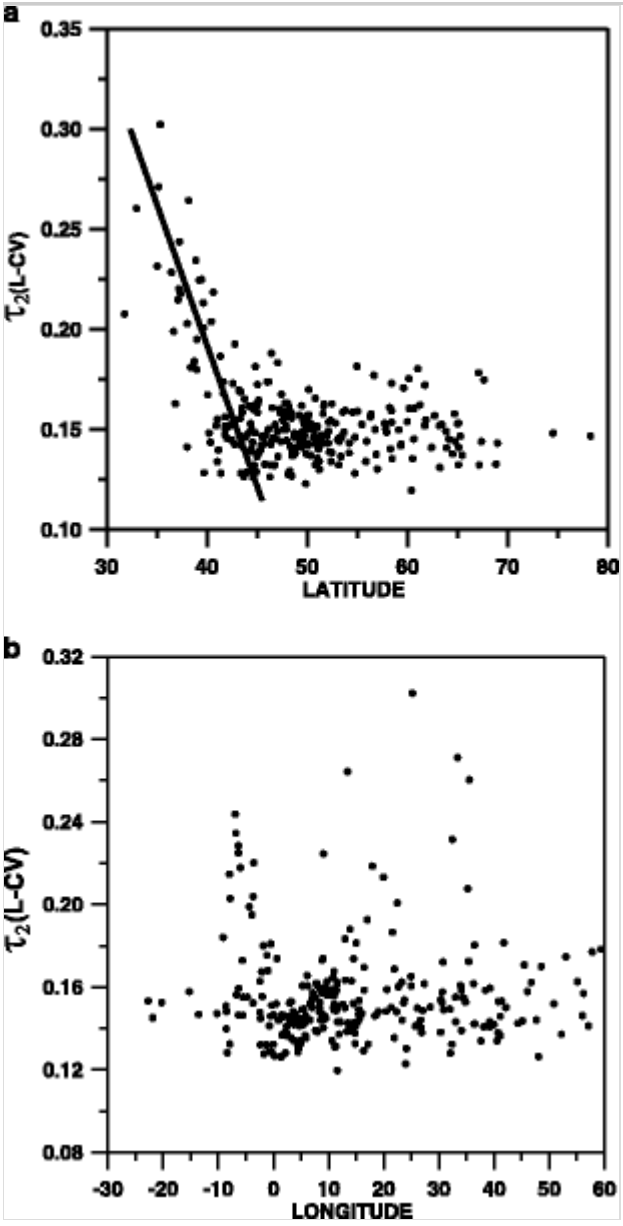

4. Discussion of the results

4.1. Database shortcomings

As previously mentioned, the available database to analyse PDS of DSL in

Europe has two shortcomings, which have to be discussed in order to assess their possible influence on the quality and reliability of the results.

The first shortcoming is the sparse distribution of rain gauges in some European areas. Consequently, outstanding spatial gradients on the different parameters of PDS distributions are debatable for the southeastern Mediterranean (Turkey and Israel). This weakness is also detected, but with moderate extent, for other areas as Greece and the Italian Peninsula. In spite of the low spatial data resolution of these areas, the results manifest a clear change on the properties of PDS parameters south of 40–45° N, strongly suggesting a climate characterised by frequent long droughts, especially for the southeastern Mediterranean.

The second shortcoming is the presence of nine rain gauges with a minimum daily rain amount equal to 1.0 mm/day and another one with 0.2 mm/day (Fig. 1), instead of the standard value of 0.1 mm/day. Unfailingly, this irregularity leads to an overestimation of some DSL, especially for 1.0 mm/day, and the results concerning these nine rain gauges could be debatable. Signs of some spatial incoherency in some clusters (Section 3.3) could be attributable to this fact due to long DSL erroneously overestimated for some rain gauges. Nevertheless, when comparing Fig. 1 (with solid circles representing the pluviometers with a minimum daily rain amount exceeding 0.1 mm/day) with the regionalization shown in Fig. 11, it is concluded that these rain gauges pertain to cluster 1, having a clear spatial coherency and homogeneity.

4.2. Threshold chosen for generating PDS

Instead of the AES procedure, the PDS strategy has been proposed to improve the distribution of long events and the corresponding return periods. Whereas AES strategy is based on choosing the extreme value for every year, the PDS strategy requires the definition of a threshold to define long events. The criterion to establish this threshold is nowadays an open problem. A review of the results obtained for the 267 rain gauges, after applying the mean-excess plot technique (Beguería 2005; Lana et al. 2006a), permits to ascertain that a wide range of thresholds would be necessary for the different rain gauges. This result should be expected, given the strong climatic differences between northern and southern latitudes or between Atlantic and Mediterranean domains. Nevertheless, these thresholds are found to be concentrated within the 92–98th percentile range,

being finally chosen then a common 95th percentile for all DSL series. In short, the threshold to define every PDS is not an arbitrary decision but a consequence of the detailed analysis of results derived from the mean-excess plot application to every one of the 267 series.

4.3. Statistical models

In terms of the L-moment formulation (Hosking and Wallis 1997), taking advantage of their robust parameter estimation and the L-skewness and L-kurtosis diagrams, two very important objectives are achieved. First, the best-fitting statistical model can be easily selected and, after that, checked by the Kolmogorov-Smirnov test. Second, the values of scale, shape and location parameters of the chosen distribution are accurately estimated. It is worth mentioning the high ratio of PDS distributed according a GP model, with just four series (at southeastern Mediterranean) departing from this model. Two of them, modelled by the GEV distribution, have the longest $L_{\max}$ of the whole set of stations (Table 4). For the other two, according to the L-skewness and L-kurtosis diagram, a specific statistic model is quite difficult to be assigned. It must be underlined that these four daily rain amount series do not belong to the set of ten rain gauges with minimum rain amount exceeding 0.1 mm/day. Consequently, the behaviour of these four series should be attributable to their climatic characteristics but not to instrumental deficiencies.

AQ13

4.4. Return periods

Assuming that the L-moments estimation leads to obtain a good fit of the empiric PDS to the GP distribution, theoretic return period values have to be accepted as a good approach to real expected long DSL for the forthcoming decades. In agreement with return period maps of 2, 5, 10, 25 and 50 years, a well-established difference is detected, with respect to the 40–45° N fringe, between northern latitudes, with DSL reaching 30–50 days, and southern latitudes, with DSL exceeding 190 days in some places. The latitudinal evolution of return periods in Europe would be in agreement with results concerning drought and rain amount trends from the IPCC-2013 (Hartmann et al. 2013).

4.5. Clustering

The possibility of some artificial groups generated by the clustering algorithm could not be discarded. It would be advisable to reconsider some of the clusters, especially the smallest, according to spatial vicinity among them and similar L-moments and scale, shape and location parameters. Particularly, couples of clusters (6, 7), (8, 9) and (4, 10) could be grouped into three clusters (Table 4 and Fig. 11). Whereas joining singular clusters 6 and 7 could be coherent, as the above-mentioned conditions are fulfilled, merging clusters (8, 9) and (4, 10) into two new clusters is a bit more questionable. Even though constraints concerning vicinity and similar L-moments and statistical parameters are quite good fulfilled, parent distributions for clusters 8 and 9 (Fig. 13) show clear DSL discrepancies, exceeding approximately 60–70 days, when comparing them with the other parent distributions. A similar behaviour is detected for clusters 4 and 10. In short, after reviewing Fig. 11 and results summarised in Table 4, two out of the three possible fusions in the Mediterranean region should be discarded. With respect to the parent distribution, it is relevant to observe the very different behaviour of cluster 1 (covering north of 40° N) with respect to the rest of distributions (Fig. 13) associated with clusters for latitudes south of 40° N.

4.6. Future scenarios for the Mediterranean area

In contrast with a notable spatial homogeneity of the PDS regime north of 40–45° N, a more complex spatial distribution south of these latitudes is quite evident. This pattern is evidenced by sharp changes on many parameters derived from the PDS analysis of the DSL. Among them, 95th percentiles of DSL, $L_{\max}$, parameters α and ξ of the GP distribution, factor score maps obtained after a rotated principal component analysis, return values of DSL for 2, 5, 10, 25 and 50 years and the spatial distribution of clusters have to be cited. The poor rain gauge coverage of the southeastern Mediterranean makes a bit more questionable to asses a different PDS regime for the southeastern Mediterranean in comparison with the western Mediterranean.

In spite of these shortcomings, different studies warn about an evident increase of dryness throughout the Mediterranean in the last century and in the next future. A change in wintertime Mediterranean precipitation toward drier conditions has likely occurred over 1902–2010, with 10 of the 12 driest winter months in just the last 20 years (Hoerling et al. 2012). This increase of dryness is also detected by analysing time trends of $L_{\max}$ at annual and seasonal scales

for years 1950–2000 (Serra et al. 2014). Different projected changes of dry periods for the Mediterranean region by the end of twenty-first century under different scenario assumptions point to significant increases in drought frequencies (Lehner et al. 2006), with increases of the maximum DSL (Hertig et al. 2012) and a northward extension of dry and arid lands, particularly in the central and southern portions of the Iberian, Italian, Hellenic and Turkish peninsulas and in areas of southeastern Europe (e.g. Romania and Bulgaria), the Middle East, northern Africa and major Islands (Corsica, Sardinia and Sicily) (Gao and Giorgi 2008). These long-term DSL projections are consistent with daily precipitation change projections for the Mediterranean region, with a pronounced decrease in precipitation, especially in the warm season (Giorgi and Lionello 2008).

5. Conclusions

Daily rainfall series for 267 European rain gauges have permitted a detailed analysis of PDS distribution of DSL. These statistics are the continuation of previous European dry spell regime studies, which were based on the ADS strategy (Serra et al. 2013), including a clustering process and time trend analysis (Serra et al. 2014). The main conclusions with respect to the PDS strategy are the following.

1. The L-moment formulation and the L-skewness and L-kurtosis diagram permit to verify that PDS of DSL are well described by the GP distribution, except for a few rain gauges at the southeastern Mediterranean.

2. Reliability of DSL return values obtained from the PDS strategy is higher than that derived from ADS, in agreement with Figs. 7 and 8 and Table 2. Discrepancies between empirical and theoretical DSL values for the PDS strategy range from −10 to +10 % throughout Europe, only reaching values close to ±20 % for a return period of 50 years, whereas for the ADS strategy, relative differences are higher and sometimes outstanding. If the ADS strategy was considered instead of the PDS method, underestimation would reach percentages exceeding 20 % for return periods of 2, 5, 10 and 25 years, reaching 40 % in small areas for a return period of 50 years. This pattern is quite common in southern Europe, whatever the return period, except for a few places.

3. The results of the PCA applied to the four first L-moments manifest the strong correlation between ℓ_1 and ℓ_2. The first rotated principal component, explaining 48 % of data variance, substitutes both L-moments. The third and fourth L-moments are strongly correlated with the second and third principal components, respectively (approximately 25.9 % of data variance for every RPC).

4. The clustering process is achieved by removing the redundant information of the two first L-moments, taking as representative variables the three FS instead of the original L-moments.

5. The regionalization process, leading to the definition of 11 clusters, manifests the presence of a high number of rain gauges (241) belonging to cluster 1 and emphasising the strong homogeneity of the PDS regime for a wide European domain. This cluster covers latitudes north of 40° N. The rest of clusters are smaller (containing one to seven rain gauges), due to the strong heterogeneity of the DSL regime for latitudes south of 40° N.

6. From the 11 clusters obtained, numbers 4 (seven rain gauges) and 11 (five rain gauges) could be assumed as the most homogeneous and confidently associated with a regional parent GP distribution. The reliability of the parent distribution for cluster 1 is quite questionable. Nevertheless, remembering the high number of rain gauges and the area covered, the possibility of a GP distribution with a single set of regional parameters could be a way to simplify the North-European DSL regime without introducing remarkable errors.

7. The analyses of the evolution of the L-CV moment with rain gauge latitudes show clear evidence of a linear increase of this parameter with decreasing latitudes south of 40–45° N. This behaviour would be in agreement with detected spatial gradients of GP parameters from north to south, 95th DSL percentiles, the longest empirical DSL, return period maps and FS of the PCA applied to the first four L-moments.

In short, the results obtained from PDS have permitted a complete description of the extreme DSL regime in Europe, highlighting the spatial homogeneity of this regime for a great part of Europe, north of 40° N, and a high heterogeneity for

southern Mediterranean regions, including a few PDS departing from the common GP model.

Acknowledgments

The authors are indebted to the European Climatic Assessment and Dataset (ECA&D) and Agencia Estatal de Meteorología, Spanish Government (AEMET) by making available pluviometric records. We also recognise the valuable comments of the reviewers.

References

Anagnostopoulou C, Maheras P, Karacostas T, Vafiadis M (2003) Spatial and temporal analysis of dry spells in Greece. Theor Appl Climatol 74:77–91

Ashkar F, Tatsambon CN (2007) Revisiting some estimation methods for the generalized Pareto distribution. J Hydrol 346:136–143

Beguería S (2005) Uncertainties in partial duration series modelling of extremes related to the choice of the threshold value. J Hydrol 303:215–230

Benjamin JR, Cornell CA (1970) Probability, statistics and decision for civil engineers. McGraw-Hill, New York

Ben-Zvi A (2009) Rainfall intensity–duration–frequency relationships derived from large partial duration series. J Hydrol 367:104–114

Berger A, Goossens C (1983) Persistence of wet and dry spells at Uccle (Belgium). J Climate 3:21–24

Brunetti M, Maugeri M, Nanni T, Navarra A (2002) Droughts and extreme events in regional daily Italian precipitation series. Int J Climatol 22(5):543–558

Carvalho JRP, Assad ED, Evangelista SRM, Pinto HS (2013) Estimation of dry spells in three Brazilian regions—analysis of extremes. Atmos Res 132–133:12–21

Cindrić K, Pasarić Z, Gajić-Čapka M (2010) Spatial and temporal analysis of dry spells in Croatia. Theor Appl Climatol 102:171–184

Coles S (2001) An introduction to statistical modelling of extreme events. Springer Series in Statistics. Springer, Germany

Davis RE, Kalkstein LS (1990) Development of an automatic spatial synoptic climatological classification. Int J Climatol 10:769–794

Davison AC, Smith RL (1990) Models for exceedances over high thresholds. J R Stat Soc Ser B 52:393–442

Dixon WJ (1985) BMDP: biomedical computer program. UCLA, Los Angeles

Douguédroit A (1987) The variation of dry spells in Marseilles from 1865 to 1984. J Climatol 7:541–551

Ekanayake ST, Cruise JF (1993) Comparison of Weibull—an exponential-based partial duration stochastic flood models. Stoch Hydrol Hydraul 7:283–297

Galloy E, Martin S, Le Breton A (1982) Analyse de séquences de jours secs consécutifs. Application à 31 postes du réseau météorologique français. La Météorologie 28:5–24

Gao X, Giorgi F (2008) Increased aridity in the Mediterranean region under greenhouse gas forcing estimated from high resolution simulations with a regional climate model. Glob Planet Chang 62:195–209

Giorgi F, Lionello P (2008) Climate change projections for the Mediterranean region. Glob Planet Chang 63:90–104

Gong DY, Wang JA, Han H (2005) Trends of summer dry spells in China during the late twentieth century. Meteorol Atmos Phys 88:203–214

Groisman PY, Knight RW (2008) Prolonged dry episodes over the conterminous United States: new tendencies emerging during the last 40 years. J Climate 21:1850–1862

Hartmann DL, Klein Tank AMG, Rusticucci M, Alexander LV, Brönnimann S, Charabi Y, Dentener FJ, Duglokencky EJ, Easterling DR, Kaplan A, Soden BJ, Thorne PW, Wild M, Zhai PM (2013) Observations: atmosphere and surface. In: Stoker TF, Qin D, Plattner GK, Tignor M, Allen SK, Boschung J, Nauels A, Xia Y, Bex V, Midgley PM (eds) Climate change 2013: the physical science basis. Contribution of Working Group I to the Fifth Assessment Report of the Intergovernmental Panel of Climate Change. Cambridge University Press, Cambridge

Heinrich G, Gobiet A (2011) The future of dry and wet spells in Europe: a comprehensive study based on the ENSEMBLES regional climate models. Int J Climatol 32:1951–1970

Hertig E, Seubert S, Paxian A, Vogt G, Paeth H, Jacobeit J (2012) Changes of total versus extreme precipitation and dry periods until the end of the twenty-first century: statistical assessment for the Mediterranean area. Theor Appl Climatol. doi: 10.1007/s00704-012-0639-5

Hoerling M, Eischeid J, Perlwitz J, Quan X, Zhang T, Pegion P (2012) On the increased frequency of Mediterranean drought. J Climate 25:2146–2161

Hosking JRM, Wallis JR (1997) Regional frequency analysis. An approach based on L-moments. Cambridge University Press, Cambridge, 224 pp

Jolliffe IT (1986) Principal components analysis. Springer series in statistics. Springer Verlag, New York, 271

Kalkstein LS, Tan G, Skindlov JA (1987) An evaluation of three clustering procedures for use in synoptic climatological classification. J Clim Appl Meteorol 26:717–730

Klein Tank AMG, Wijngaard JB, Können GP, Böhm R, Demarée G, Gocheva A, Mileta M, Pashiardis S, Hejkrlik L, Kern-Hansen C, Heino R, Bessemoulin P, Müller-Westermeier G, Tzanakou M, Szalai S, Pálsdóttir T, Fitzgerald D, Rubin S, Capaldo M, Maugeri M, Leitass A, Bukantis A, Aberfeld R, Van Engelen AFV, Forland E, Mietus M, Coelho F, Mares C, Razuvaev V, Nieplova E, Cegnar T, Antonio López J, Dahlström B, Moberg A, Kirchhofer

W, Ceylan A, Pachaliuk O, Alexander LV, Petrovic P (2002) Daily dataset of 20th century surface air temperature and precipitation series for the European climate assessment. Int J Climatol 22:1441–1453

Klok EJ, Klein Tank AMG (2009) Updated and extended European dataset of daily climate observations. Int J Climatol 29:1182–1191

Kostopoulou E, Jones PD (2005) Assessment of climate extremes in the Eastern Mediterranean. Meteorog Atmos Phys 89:69–85

Kutiel H (1985) The multimodality of the rainfall course in Israel as reflected by the distribution of dry spells. Arch Met Geoph Biocl Ser B 36:15–27

Kutiel H, Maheras P (1992) Variations interannuelles des séquences sèches et des situations synoptiques en Méditerranée. Publ l'AIC 5:15–27

~~Lana X, Burgueño A (1998a) Daily dry-wet behaviour in Catalonia (NE Spain) from the viewpoint of first and second order Markov chains. Int J Climatol 18(7):793–815~~

AQ14

~~Lana X, Burgueño A (1998b) Probabilities of repeated long dry episodes based on the Poisson distribution. An example for Catalonia (NE Spain). Theor Appl Climatol 60:111–120~~

AQ15

Lana X, Burgueño A, Martínez MD, Serra C (2006a) Statistical distributions and sampling strategies for the analysis of extreme dry spells in Catalonia (NE Spain). J Hydrol 324:94–114

Lana X, Martínez MD, Burgueño A, Serra C, Martín-Vide J, Gómez L (2006b) Distributions of long dry spells in the Iberian Peninsula, years 1951–1990. Int J Climatol 26:1999–2001

Lana X, Martínez MD, Burgueño A, Serra C (2008a) Return period maps of dry spells for Catalonia (North-eastern Spain) based on the Weibull distribution. Hydrol Sci J 53(1):48–64

Lana X, Martínez MD, Burgueño A, Serra C, Martín-Vide J, Gomez L (2008b) Spatial and temporal patterns of dry spell lengths in the Iberian Peninsula for the second half of the twentieth century. Theor Appl Climatol 91:99–116

Lana X, Burgueño A, Martínez MD, Serra C (2012) Some characteristics of daily rainfall déficit regime base on the dry day since last rain (DDSLR) index. Theor Appl Climatol 109:153–174

Leander R, Buishand TA, Klein Tank AMG (2014) An alternative index for the contribution of precipitation on very wet days to the total precipitation. J Climate 27:1365–1378

Lehner B, Dölh P, Alcamo J, Henrichs T, Kaspar F (2006) Estimating the impact of global change on flood and drought risks in Europe: a continental integrated analysis. Climate Change 75:273–299

Lemeshko BY, Postokalov SN (2001) Application of the non parametric goodness-of-fit test in testing composite hypothesis. Optoelectron Instrum Data Process 2:76–88

Llano MP, Penalba OC (2011) A climatic analysis of dry sequences in Argentina. Int J Climatol 31:504–513

Madsen H, Pearson CP, Rosbjerg D (1997a) Comparison of annual maximum series and partial duration series method for modeling extreme hydrologic events: 2. Regional modeling. Water Resour Res 33:759–769

Madsen H, Rasmussen PF, Rosbjerg D (1997b) Comparison of annual maximum series and partial duration series method for modeling hydrologic events: 1. At site modeling. Water Resour Res 33:747–757

Mailhot A, Lachance-Cloutier S, Talbot G, Favre AC (2013) Regional estimates of intense rainfall based on the Peak-Over-Threshold (POT) approach. J Hydrol 476:188–199

Martín-Vide J, Gómez L (1999) Regionalization of peninsular Spain based on

the length of dry spells. Int J Climatol 19:537–555

Miquel J (1984) Guide pratique d'estimation des probabilités de crues. Ed. Eyrolles, Paris, 160 pp

Nastos PT, Zerefos CS (2009) Spatial and temporal variability of consecutive dry and wet days in Greece. Atmos Res 94:616–628

Perzyna G (1994) Spatial and temporal characteristics of maximum dry spells in Southern Norway. Int J Climatol 14:895–909

Preisendorfer RW (1988) Principal component analysis in meteorology and oceanography. Development in atmospheric sciences, 17. Elsevier, Amsterdam, 435 pp

Rosjberg D, Rasmussen PF, Madsen H (1991) Modelling of exceedances in partial duration series. International Hydrology and Water Resources Symposium. Inst. of Eng., Perth

Sánchez E, Domínguez M, Romera R, López de la Franca N, Gaertner MA, Gallardo C, Castro M (2011) Regional modeling of dry spells over the Iberian Peninsula for present climate and climate change conditions. Climate Change 107:625–634

Sarhadi A, Heydarizadeh M (2014) Regional frequency analysis and spatial pattern characterization of dry spells in Iran. Int J Climatol 34:835–848

Schmidli J, Frei C (2005) Trends of heavy precipitation and wet and dry spells in Switzerland during the 20th century. Int J Climatol 25:753–771

Serra C, Burgueño A, Martínez MD, Lana X (2006) Trends in dry spells across Catalonia (NE Spain) during the second half of the 20th century. Theor Appl Climatol 85:165–183

Serra C, Martínez MD, Lana X, Burgueño A (2013) European dry spell length distributions, years 1951–2000. Theor Appl Climatol 114:531–551

Serra C, Martínez MD, Lana X, Burgueño A (2014) European dry spell

regimes (1951–2000): clustering process and time trends. Atmos Res 144:151–174

She D, Xia J, Song J, Du H, Chen J, Wan L (2013) Spatio-temporal variation and statistical characteristic of extreme dry spell in Yellow River Basin, China. Theor Appl Climatol 112:201–213

Sivakumar MVK (1992) Empirical analysis of dry spells for agricultural applications in West Africa. J Climate 5:532–539

Tallaksen LM, Madesn H, Hisdal H (2004) Frequency analysis. In: Tallaksen LM, Van Lanen HAJ (eds) Hydrological drought. Processes and estimation methods for streamflow and groundwater, Developments in Water Science (48). Elsevier, Amsterdam

Vicente-Serrano SM, Beguería S (2003) Estimating extreme dry-spell risk in the middle Ebro Valley (North-eastern Spain): a comparative analysis of partial duration series with a Pareto distribution and annual maxima series with a Gumbel distribution. Int J Climatol 23:1103–1118

Wijngaard JB, Klein Tank AMG, Konnen GP (2003) Homogeneity of 20th century European daily temperature and precipitation series. Int J Climatol 23:679–692

Zolina O, Simmer C, Konstantin B, Sergey KG, Peter K (2013) Changes in the duration of European wet and dry spells during the last 60 years. J Climate 26:2022–2047